© 2018. Published by The Company of Biologists Ltd | Journal of Experimental Biology (2018) 221, jeb177972. doi:10.1242/jeb.177972

RESEARCH ARTICLE

Photoreceptor specialization and the visuomotor repertoire of the primitive chordate *Ciona*

Priscilla Salas[1], Vall Vinaithirthan[1], Erin Newman-Smith[1], Matthew J. Kourakis[2] and William C. Smith[1,2,*]

ABSTRACT

The swimming tadpole larva of *Ciona* has one of the simplest central nervous systems (CNSs) known, with only 177 neurons. Despite its simplicity, the *Ciona* CNS has a common structure with the CNS of its close chordate relatives, the vertebrates. The recent completion of a larval *Ciona* CNS connectome creates enormous potential for detailed understanding of chordate CNS function, yet our understanding of *Ciona* larval behavior is incomplete. We show here that *Ciona* larvae have a surprisingly rich and dynamic set of visual responses, including a looming-object escape behavior characterized by erratic circular swims, as well as negative phototaxis characterized by sustained directional swims. Making use of mutant lines, we show that these two behaviors are mediated by distinct groups of photoreceptors. The *Ciona* connectome predicts that these two behavioral responses should act through distinct, but overlapping, visuomotor pathways, and that the escape behavior is likely to be integrated into a broader startle behavior.

KEY WORDS: Behavior, Connectome, Phototaxis

INTRODUCTION

The sub-phylum of the chordates known as the tunicates are the closest living relatives of the vertebrates (Delsuc et al., 2006). The close evolutionary relationship between vertebrates and tunicates is most evident in the tunicate tadpole larva. Tunicate larvae have been the subject of intensive research stretching back well over 100 years (for comprehensive reviews, see Satoh, 1994, 2014). While considerable variation in form and size is found among larvae of the thousands of tunicate species, those of the widely studied *Ciona* species of ascidian exemplify the larval body plan. Although scarcely 1 mm in length and containing less than 1600 cells (Nakamura et al., 2012), the *Ciona* larval tadpole has a stereotyped chordate body plan with a long tail dominated by a central 40-cell notochord and 36 flanking muscle cells. Anterior to the tail, the trunk contains the larval brain, as well as the precursors of the circulatory and digestive systems.

The ascidian larval central nervous system (CNS) develops from a dorsal neural plate in a manner homologous to vertebrates (Hashimoto et al., 2015) and, once formed, three distinct regions in the CNS are recognized (Ikuta and Saiga, 2007): the brain vesicle (BV; sometimes called the sensory vesicle because of the presence of several sensory systems in this region), the motor ganglion (MG; sometimes called the visceral ganglion) and a tail nerve cord. The structure, function and genes expressed within the various domains of the CNS have allowed tentative anatomical homologs to vertebrate CNS regions to be identified (reviewed in Hudson, 2016). The brain vesicle has been equated with the vertebrate forebrain, while the motor ganglion, with its 5 pairs of cholinergic motor neurons, and the tail nerve cord, which gives rise to a pair of neural crest cells (Stolfi et al., 2015), have been equated with the vertebrate spinal cord and/or hindbrain. The narrow neck region joining the brain vesicle to the motor ganglion appears to be homologous to the vertebrate midbrain/hindbrain junction. Despite this conservation with a generalized vertebrate CNS, *Ciona* larvae have only 177 neurons in the CNS, and several dozen in the peripheral nervous system (PNS) (Ryan et al., 2018).

Although the larval stage of *Ciona* lasts for only a few days, it is nevertheless a critical period during which the larva finds and attaches to a suitable substrate where it will undergo metamorphosis and spend the remainder of its ∼1 year life. *Ciona* larvae swim freely in the ocean and rely on several sensory systems to navigate, detect substrates and perhaps avoid predation. In its search for a home, the larva is aided by visual, geotactic, tactile and possibly chemosensory inputs. Despite the short larval stage, behaviors such as geotaxis and phototaxis are temporally dynamic (Kajiwara and Yoshida, 1985; Svane and Young, 1989; Zega et al., 2006). Two well-studied sensory systems are found in the brain vesicle: one responds to light (the ocellus) and the other to gravity (the otolith) (Tsuda et al., 2003b); a third possible sensory system in the brain vesicle is composed of the coronet cells (Moret et al., 2005; Ryan et al., 2016). The major component of the otolith is a single pigmented cell tethered to the base of the brain ventricle and contacting two antenna sensory neurons. By monitoring the movement of the pigment cell in the ventricle, the larva is able to orient itself with respect to gravity (Sakurai et al., 2004). The ocellus is a more complex organ, composed of two distinct groups of Ci-opsin1-expressing ciliary photoreceptors (Ryan et al., 2016; Eakin and Kuda, 1971; Horie et al., 2008b): Group I and II photoreceptors. Group I photoreceptors are the most abundant, with 23 cells in all. The bodies of these cells surround and extend their outer segments into the cup-shaped ocellus pigment cell. Light is directed to the cup, and thus to the Group I photoreceptors, via three anteriorly situated lens cells, while the surrounding pigment cell shades the photoreceptors from light not passing through the lens cells. The Group II photoreceptors are found adjacent and anterior to the Group I photoreceptors. The Group II cluster contains only seven cells, and the outer segments extend into a protrusion in the brain ventricle rather than into the pigment cell (i.e. they are not shaded and should be receptive to light from all directions). A third group of photoreceptors is found outside of the ocellus at the posterio-ventral wall of the brain vesicle. The function of the Group III photoreceptors is unknown, but they appear to play no role in the known photoresponses (Horie et al., 2008a,b), and they make very

[1]Department of Molecular, Cell and Developmental Biology, University of California, Santa Barbara, Santa Barbara, CA 93106, USA. [2]Neuroscience Research Institute, University of California, Santa Barbara, Santa Barbara, CA 93106, USA.

*Author for correspondence (w_smith@lifesci.ucsb.edu)

W.C.S., 0000-0002-6257-7695

Received 23 January 2018; Accepted 22 February 2018

few synaptic connections, unlike the Group I and II photoreceptors (Ryan et al., 2016). In addition to these central sensory systems, *Ciona* larvae have an extensive PNS consisting of several classes of single ciliated nerve cells in the epidermis which transduce mechanical, and perhaps chemical, stimuli (Ryan et al., 2018).

The visuomotor responses of ascidian larvae have been the subject of a number of studies stretching back nearly a century (Grave, 1920; Mast, 1921). Several species of ascidian have been studied and behaviors including responses to rapid light dimming (the dimming or shadow response), as well as negative and positive phototaxis have been described (Kajiwara and Yoshida, 1985; Svane and Young, 1989; Zega et al., 2006; Tsuda et al., 2003a,b; Grave, 1920; Mast, 1921; McHenry, 2005; Young and Chia, 1985). Nevertheless, ascidian larval visuomotor behavior remains poorly understood, and descriptions of ascidian larval behavior have often been generalized from studies across diverse species, despite apparent species differences (McHenry, 2005; Young and Chia, 1985). Moreover, there is little agreement in the literature concerning the functions, and possible relationship, of the phototactic and dimming behaviors. While these two behaviors have sometimes been described as distinct and independent (Kajiwara and Yoshida, 1985), elsewhere the dimming response has been proposed as a component of phototaxis (Zega et al., 2006; Mast, 1921; McHenry, 2005), or even as an experimentally provoked response that mimics phototactic cues (Young and Chia, 1985).

The recent completion of the *Ciona* larval connectome (Ryan et al., 2016) encourages a fuller understanding of *Ciona* larval behavior with the goal of finding neural-network correlates of behaviors. The *Ciona* connectome describes a highly asymmetrical CNS, which includes left-biased visuomotor pathways. The present study was undertaken with the hypothesis that the negative phototaxis and dimming response behaviors are distinct and serve different functions. Moreover, we hypothesize that the Group I and Group II photoreceptors mediate these two behaviors, respectively. In support of these hypotheses, we describe here two distinct light-induced responses: one that is characterized by asymmetric (i.e. circular) swimming in response to dimming light that appears to function as an escape mechanism, and another, later-developing, phototaxic response to continuous directional light that results in symmetric (i.e. straight) swimming. Moreover, we show with the aid of a mutant albino line that Group I photoreceptors predominantly mediate symmetric swims, and Group II asymmetric swims. Finally, we discuss how the divergent descending pathways from the two photoreceptor groups derived from the *Ciona* connectome relate to our behavioral observations.

MATERIALS AND METHODS

Animals

Note on species names: in the past couple of years, it has been brought to the attention of the *Ciona* research community that animals previously identified as *Ciona intestinalis* may in fact be one of either of two species – *Ciona robusta* or *Ciona intestinalis* (Brunetti et al., 2015). Previously, these have been called *C. intestinalis* type A and B, respectively (Caputi et al., 2007). The range of *C. robusta* is much broader and, accordingly, much of the published literature reporting to be on *C. intestinalis* is instead on *C. robusta*. By contrast, the recently published *Ciona* larval connectome (Ryan et al., 2016) is for a *C. intestinalis*.

Adult *C. robusta* (also known as *C. intestinalis*, type A) were collected from the Santa Barbara Harbor and either used immediately or cultured at the UC Santa Barbara Marine Lab. Adult *C. intestinalis* (also known as *C. intestinalis* type B) were obtained from the Marine Biological Laboratory (Woods Hole, MA, USA).

Ciona larvae were obtained by mixing gametes of 3 or more adults, as described previously (Veeman et al., 2011). All embryos and larvae were cultured in natural seawater at 18°C. Larvae age is given as hours post-fertilization (hpf).

The *C. robusta* mutant *pristine* (*prs*) was identified from the wild Santa Barbara population by self-fertilization. The mutant was expanded by outcrossing to wild-type animals and maintained at the UC Santa Barbara marine lab. To produce homozygous *prs* adults, albino larvae produced by the crossing of two heterozygous *prs* adults were isolated, settled on Petri dishes and cultured until adults. To test for complementation to other *Ciona* albino lines, *prs* eggs were chemically dechorionated and then mixed with sperm from either of two *Ciona savignyi* mutant strains, *spotless* or *immaculate* (Jiang et al., 2005). All *Ciona* genetic methods are as described previously (Veeman et al., 2011). Arrestin staining of larvae was done as described previously (Jiang et al., 2005).

Behavioral assays

End-point assay for phototaxis

Fertilized eggs in seawater were placed in the inverted lids of 10 cm Petri dishes with the bottom section floating on top, allowing larvae to settle on the underside, as described previously (Veeman et al., 2011). The floating bottom section was secured with a small piece of tape so that it would remain fixed during the assay. Both a broad-spectrum 23 W compact fluorescent light [Feit Electric CE23TM/4(N), Pico Rivera, CA, USA] and a fiber optic microscope illuminator (Leica, Wetzlar, Germany) fitted with a 150 W halogen light bulb (Osram, Munich, Germany) were tested for stimulating phototaxis, and were found to be equally effective at the same range of intensities.

The light sources were placed to one side of, and 25 cm above, the dish. The dishes were placed at various distances from the light, and light intensities (lux) were measured at the center of the Petri dishes with a Traceable Dual-Range Light Meter (Fisher Scientific, Waltham, MA, USA). At the end of 3 days, the sea water was decanted from the plates and the attached larvae (referred to as juveniles) were stained for 30 min with 0.1% Coomassie Blue in 10% acetic acid and 50% methanol, and then washed in 10% acetic acid and 50% methanol. The stained plates were photographed and the attached juveniles counted.

Live phototaxis and dimming response assays

Images were collected with a Hamamatsu ORCA-flash4.0 camera (Hamamatsu City, Japan) fitted on either an Olympus SX12 stereomicroscope (Tokyo, Japan) or a macro zoom lens (Navitar 7000, Rochester, NY, USA). White light was delivered using the fiber optic illuminator, and illumination intensities were determined as described above for the end-point assay. To image larval behavior in lights-off assays, as well as in dark-adapted conditions, larvae were illuminated with far-red light, as described previously (Tsuda et al., 2003a,b), using a Kodak GBX-2 safelight and a red barrier filter (Olympus SZX2-MRFP) in the imaging light path.

Data analysis and statistical measures

Tail flick and sustained swim criteria

Swims were counted as tail flicks if a larva was initially stationary and no more than four beats of the tail were counted. All other swims were counted as sustained. Swimming behavior was scored from 1 min capture sessions at 10 frames s^{-1}. During the 1 min

imaging period larvae may (infrequently) display more than one swimming event. The number of scored swims was normalized by dividing by the total number of larvae screened in each movie. Swims resulting from one larva brushing or bumping into another were not counted. Additionally, in the course of the assays, some larvae became trapped at the air/water interface; these larvae were evident by their focal plane and their stationary position despite tail beating, and were not counted or scored.

Tracking and quantification of swims

Larval swims were tracked manually and measured for length, angle of net trajectory and tortuosity using ImageJ (Schneider et al., 2012).

Sampling

Quantification of larvae swim parameters was done using a minimum of three independent movies. To avoid biased sampling in our analysis of larval swim events, characteristics of all larvae in the field of view from multiple movies were analyzed or, if the field of view contained too many larvae to score, it was divided into equal segments (typically 12) and a random number generator was used to choose a segment to be analyzed.

Tests of significance

In most cases, we calculated significance using Student's *t*-test, comparing quantified responses between multiple imaging sessions. The exception to this was calculation of differences in swim tortuosity and angle, which did not show a normal distribution. In these cases, the Wilcoxon signed-rank test was used.

RESULTS

The albino mutant line *pristine* lacks phototaxis but not photosensitivity

We developed a simple and robust end-point assay to quantify the negative phototactic behavior of *C. robusta* larvae. Embryos were placed in 10 cm Petri dishes approximately 1 h after fertilization, with a floating lid to allow the larvae to attach to the underside, which is their preference (Veeman et al., 2011; see Materials and Methods). A white light source was placed to one side of the dish (termed 'directional light'), and the Petri dishes were left undisturbed for 3 days. During these 3 days the embryos developed and hatched, and the resulting larvae swam before attaching to the Petri dishes and commencing metamorphosis. At the end of 3 days, the attached larvae (referred to as juveniles at this developmental stage) were visualized by staining with Coomassie Blue. Fig. 1A shows a representative result. In this example, of 325 attached juveniles, the majority (235) were clustered at the edge furthest away from the light source (dashed oval). The remaining juveniles were found scattered, but almost exclusively on the half of the dish away from the light source. When Petri dishes where placed at progressively greater distances from the light source, with a range of illumination intensities from 130 to 1400 lx (expressed as $\log_{10}$ light intensity in Fig. 1B), the percentage of juveniles attached at the far side (i.e. away from the light), calculated from three independent trials, was found to decline with light intensity. The results show an illumination dependency in the ability of the larvae to perform negative phototaxis, with larvae in the least illuminated dish (i.e. furthest from the illumination) showing greatly reduced negative phototaxis (Fig. 1B).

In a screen for spontaneous mutants performed by self-fertilization of wild-collected *C. robusta* (Veeman et al., 2011), we identified the mutant line *pristine* (*prs*), which lacks pigmentation (melanin) in the brain vesicle (i.e. an albino; Fig. 1C). The *prs* mutation is recessive but not lethal, and adults bred to homozygosity for the *prs* mutation produced 100% albino offspring when either self-fertilized or crossed to one another. Crosses of *prs* to two previously isolated albino mutants, *spotless* (*spt*) and *immaculate* (*imm*), from the congeneric species *C. savignyi* (Jiang et al., 2005), yielded 100% pigmented hybrid larvae, indicating that the *prs* mutation is at a different gene from either *spt* or *imm*. Additionally, single nucleotide polymorphism (SNP) analysis (Veeman et al., 2011) showed that the *prs* mutation is not linked to tyrosine hydroxylase, the mutated gene in *spt* (data not shown). Although lacking melanization of the brain vesicle, *prs* larvae (*prs*/*prs*) have photoreceptors, as shown by staining for Arrestin (Horie et al., 2005; Fig. 1C). Despite the presence of photoreceptors, the *prs* larvae showed no phototactic behavior (Fig. 1D,E), supporting previous assertions that pigmentation associated with the Group I photoreceptors is required for phototaxis (Svane and Young, 1989; Mast, 1921; Jiang et al., 2005). Although lacking phototaxis, *prs* larvae responded rapidly to dimming light with a bout of swimming (Movie 1), indicating that they remained photoresponsive. To quantify this response, and to compare it with that of wild-type larvae, *prs* and wild-type larvae were scored for swimming behavior in the 5 s preceding and following dimming of the light. We observed that *prs* larvae not only responded to light dimming but in fact had an elevated response compared with wild-type larvae, which was evident when dimming the light from low levels (3 and 10 lx) (Fig. 1F). (Fig. S1 shows the responses of wild-type larvae to light dimming at a range of illuminations from 3 to 300 lx.)

Early hatching larvae lack phototactic behavior but show the dimming response

Previous reports in *C. savignyi* indicated that negative phototactic behavior was not evident until several hours after fertilization, while sensitivity to light dimming developed several hours earlier (Kajiwara and Yoshida, 1985). A fuller understanding of temporal changes in *Ciona* larval behavior will be important not only for potentially distinguishing swimming due to phototaxis and light dimming but also for the interpretation of the *Ciona* connectome data that were derived from a 21 hpf larva. In order to assess the developmental onset of negative phototaxis, the behavior of groups of ∼200 *C. robusta* larvae in 10 cm Petri dishes with directional illumination was recorded at 30 min intervals starting ∼2 h after hatching and continuing for 10.5 h (e.g. 21.2 to 31.7 hpf). The accumulation of larvae in the side of the dish away from the light (distal side) was evident when comparing representative images from the beginning and end points (Fig. 2A,B; Movie 2). Compiled results from three separate negative phototaxis assays are shown in Fig. 2C. We observed no evidence of phototaxis until ∼23 hpf.

In order to further characterize the apparent change in swimming behavior starting at approximately 23 hpf, a second set of movies with higher temporal resolution (10 frames s^{-1}) was collected at 21 and 25 hpf. Swims from 1 min movies at the two time points were assessed for the angle of the swim trajectory relative to the directional illumination, the length of the swim and the tortuosity of the swim (defined as the ratio between the length of the swim and the distance between the beginning and end points) (Fig. 2D,E). To be counted in this assay, swims had to consist of at least four beats of the tail. Fig. 2D shows the analyzed swims with direction indicated radially (180 deg corresponds to swimming directly into the light while 0 deg indicates swimming directly away), and the length of the rays indicating the swim length. In comparing 21 hpf swims

Journal of Experimental Biology (2018) 221, jeb177972. doi:10.1242/jeb.177972

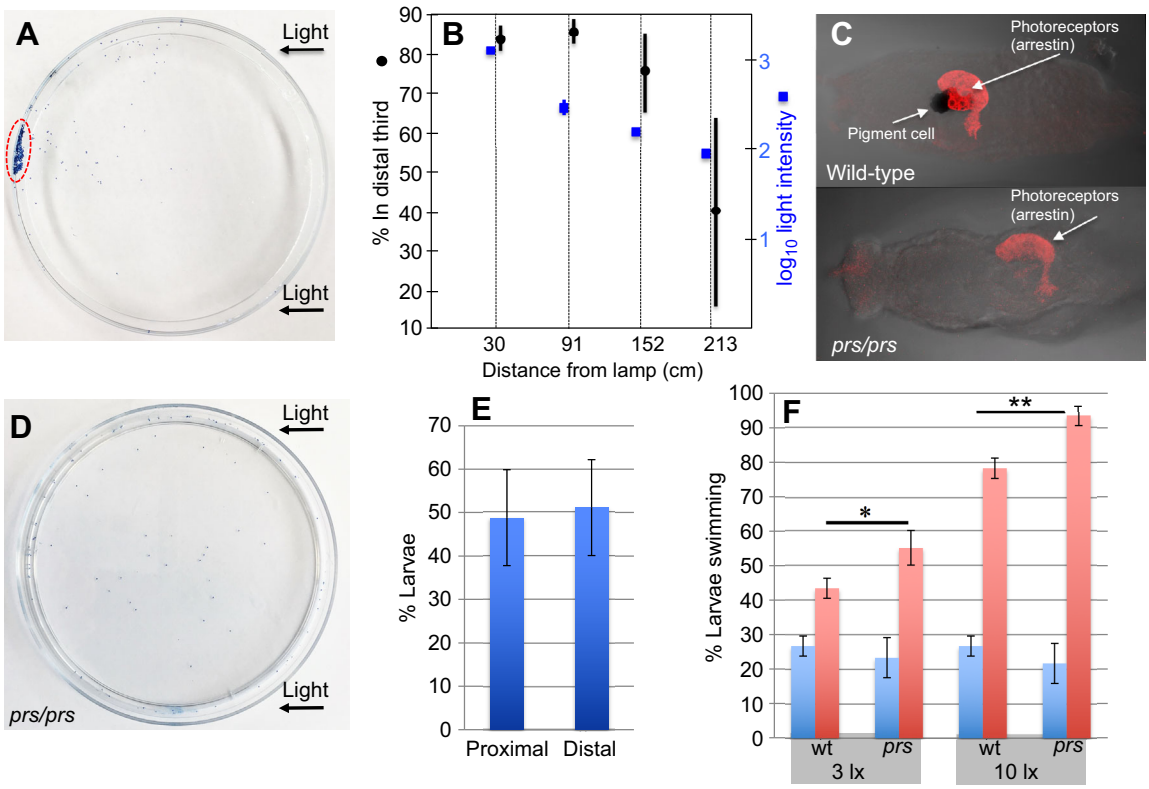

Fig. 1. Phototaxis and dimming responses in wild-type and pristine (*prs*) *Ciona robusta* mutants. (A) Coomassie Blue-stained wild-type *C. robusta* juveniles attached to a 10 cm Petri dish. The majority are clustered at the far edge (dashed oval), away from the indicated directional light. (B) Dependency of negative phototaxis in *C. robusta* on directional light intensity. Graph shows the percentage of juveniles attaching to the distal third (away from the light source) of the Petri dish from three independent trials as a function of directional light intensity (lx). Points are the mean from three trials (±s.d.). (C) Top panel: *C. robusta* wild-type larvae with an ocellus pigment cell and arrestin-positive photoreceptor cells indicated; bottom panel: homozygous *prs* mutant larva that is positive for arrestin but lacking pigment. (D,E) Homozygous *prs* larvae do not show negative phototaxis. (D) In a phototaxis assay, no clustering on the distal side of the Petri dish (away from the light source) was observed. (E) Percentage of *prs* larvae attaching to the distal and proximal sides of Petri dishes. Bars indicate means from three trials (±s.d.). (F) Homozygous *prs* larvae do respond to light dimming. Blue bars indicate the percentage of larvae swimming in a 5 s period prior to light dimming, while red bars indicate the percentage of larvae swimming in a 5 s period after light dimming. Shown are the means (±s.d.) from three movies, with 20 larvae assessed for each movie. **P*<0.05, ***P*<0.01 (Student's *t*-test). wt, wild-type larvae.

with 25 hpf swims, there was a significant change in the angle of swim trajectories away from the light source in the older larvae (Fig. 2D; $P<0.05$). Most interestingly, we observed a decrease in the tortuosity of swim (i.e. straighter swims) in the older larvae ($P<0.01$) (Fig. 2E). Thus, there is a qualitative change in the swims between 21 hpf and 25 hpf, resulting in straighter and more oriented swims, which appears to account for the delayed onset of negative phototaxis. Movie 3 shows a field of 25 hpf larvae recorded with directional light at 10 frames s^{-1}. Three larvae showing sustained negative phototactic swims are circled, while other larvae showing more tortuous swims are also evident.

Because the data shown in Fig. 2 were with *C. robusta* larvae, and the connectome was derived from a *C. intestinalis* larva (Ryan et al., 2016), we extended our observations to *C. intestinalis*. We observed that *C. intestinalis* larvae are also strongly negative phototactic (Fig. S2A). We also observed that when grown under identical conditions at 18°C, *C. intestinalis* hatched 1–1.5 h later than *C. robusta*. Whether this reflects an overall slower development of *C. intestinalis* remains to be determined. However, because of the delay in hatching, we assessed *C. intestinalis* swims offset 1.5 h from those of *C. robusta*. Nevertheless, we observed a large decrease in the tortuosity of *C. intestinalis* swims in directional light from 22.5 hpf to 26.5 hpf (Fig. S2B).

In contrast to the relatively late onset of negative phototaxis, the ability of *C. robusta* larvae to respond to dimming light was evident much earlier (Fig. 3). While no response was evident in newly hatched larvae (19.5 hpf), by 20.5 hpf we observed a robust response to light dimming, and a similar time course was observed in *C. intestinalis*, albeit with a delayed hatching (Fig. S2C).

Tail flicks and sustained swims are regulated independently

In order to be able to compare the swims evoked by phototaxis versus light dimming, we further characterized negative phototactic behavior in older wild-type and *prs* larvae (28.5–30 hpf; i.e. after the onset of negative phototaxis). Multiple 1 min movies were recorded at 10 frames s^{-1} with either directional or far-red illumination. *Ciona* larvae are insensitive to far-red light (Nakagawa et al., 1999), and its use for illumination will be referred to here as 'dark conditions'. We observed that at any given instant during the 1 min recording sessions the majority of the larvae were stationary, and individuals, apparently at random, would become active and show one of two behaviors that we classified as (1) tail flicks, consisting of ≤3 beats of the tail or (2) sustained swims, consisting of >3 beats of the tail. Movie 4 shows an example of each class. Fig. 4A,B shows the trajectories for all swims of a group of wild-type larvae during a 1 min directed-light capture (Movie 5) and that were classified as either sustained swims (Fig. 4A), or tail flicks (Fig. 4B). Most sustained swims (30 out of 33) resulted in net movement away from the light, which differed significantly from tail flicks, which were randomly orientated and resulted in little movement.

Journal of Experimental Biology (2018) 221, jeb177972. doi:10.1242/jeb.177972

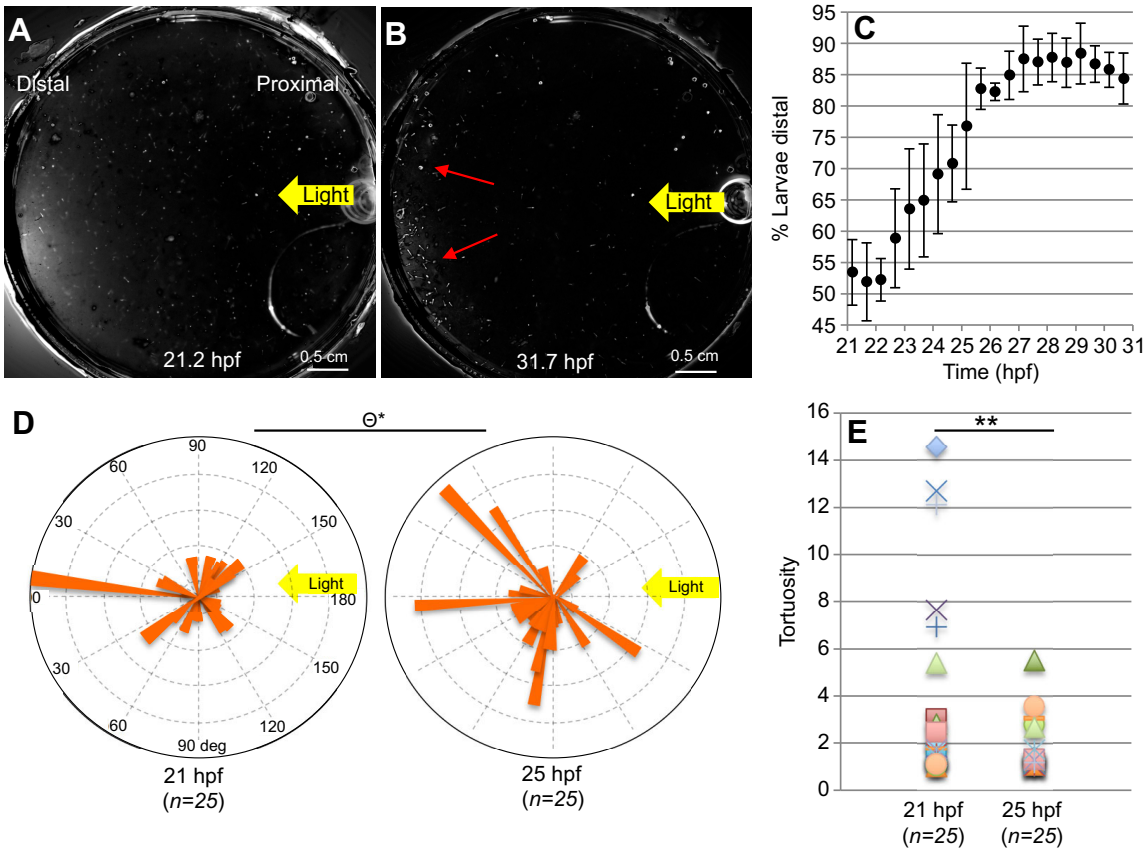

Fig. 2. Development of negative phototaxis in *C. robusta*. (A,B) Representative images showing the beginning and end points, respectively, of a negative phototaxis time-lapse recording. Yellow arrows indicate the direction of light, and red arrows in B indicate the accumulation of larvae at the distal side of the dish. (C) Graph of negative phototaxis. The percentage of larvae in the distal halves of Petri dishes measured at 30 min intervals starting at 21.2 h post-fertilization (hpf) is shown. Points indicate means from three movies (±s.d.). (D) Angles (Θ) and lengths of swims plotted in the angular and radial axes, respectively, for larvae at 21 and 25 hpf. The direction of light is indicated. (E) Tortuosity of the swims analyzed in D. For D and E: *P<0.05, **P<0.01 (Wilcoxon signed rank test).

To quantify and compare the behavior of *prs* and wild-type larvae under these different illumination conditions, three movies were scored for each condition, and all larvae in the field of view were scored in each movie. The swims were classified as sustained or tail flick, and for each movie the number of swims for each class was normalized to the total larvae scored in that movie (reported in Fig. 4C,D as events per larvae screened). In wild-type larvae under dark conditions, tail flicks predominated, with few sustained swims observed (Fig. 4C). However, when larvae from the same clutch were scored in the presence of directional light, the number of sustained swims greatly increased. The profile of swims in *prs* mutant larvae recorded in the dark closely resembled that of wild-type larvae, with tail flicks predominating. However, unlike wild-type larvae, *prs* larvae showed no increase in sustained swims in the presence of directional light. We also observed that the normalized number of tail flicks declined in light versus dark conditions for both wild-type and *prs* larvae. While it is possible that some wild-type larval swims that started as tail flicks could become sustained swims when a directional light cue was received, the observation that a similar decrease in tail flicks was observed in *prs* larvae in dark versus light conditions, without an accompanying increase in sustained swims, argues against this. Moreover, the total number of normalized wild-type swim events (tail flicks plus sustained swims) increased in light versus dark conditions (Fig. 4D; P<0.01). Thus the observations indicate that directional light not only provided directional cues but also stimulated the number of sustained swims, while inhibiting tail flicks. Taken together, these results indicate that tail flicks and sustained swims are independent swim events.

Response to light dimming is quantitatively and qualitatively different from negative phototaxis

We have observed that the phototactic and dimming responses have different developmental onsets, but that in older larvae both behaviors are present (Figs 2 and 3). This is further demonstrated in Fig. 5 (and Movie 6), in which a group of larvae swimming in continuous directional light were subjected to light dimming. Fig. 5A,B shows 5 s projection images from Movie 6 in which swims appear as white trails. Fig. 5A shows 5 s trajectories of larvae swimming in directional light (as indicated by the arrow), while Fig. 5B shows the trajectories of the same group of larvae for the first 5 s following lights-off. Not only are more larvae swimming following lights-off, but the swim characteristics appear to be qualitatively different between the two conditions, with the swims evoked by light dimming being more tortuous. Fig. 5C shows the 10 s paths of 11 randomly chosen larvae from Fig. 5B, with arrows indicating their positions relative to the light source at the time of light dimming. We observed this behavior in larvae oriented both towards and away from the light source, consistent with the dimming response being independent of light direction.

To quantify the apparent differences in swim trajectories between the two conditions, larvae exhibiting either sustained swims under continuous directional light or swims induced by light dimming

Journal of Experimental Biology (2018) 221, jeb177972. doi:10.1242/jeb.177972

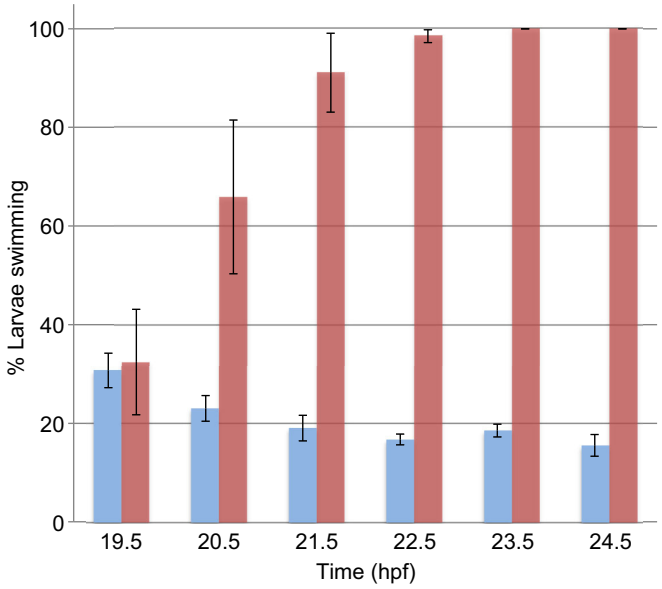

Fig. 3. Developmental time course of dimming response in *C. robusta* larvae. Blue bars indicate the percentage of larvae swimming in a 5 s period prior to light dimming, while red bars indicate the percentage of larvae swimming in a 5 s period after light dimming. Shown are the means (±s.d.) from three movies with 45 larvae assessed for each movie.

were randomly selected from a set of five movies. The degree of tortuosity for swims for each larva in the two groups was calculated and plotted (Fig. 5D). The dim group showed significantly higher tortuosity than the light group. Finally, we scored the direction of turning for larvae that swam in circles following light dimming, and the majority (82%) swam counter-clock wise (n=50), which for a larva swimming in the normal dorsal-side up position corresponds to leftward turning.

Response to light dimming is quantitatively and qualitatively different in *prs* larvae

In addition to observing that *prs* larvae are more sensitive to light dimming than wild-type larvae (Fig. 1F), further analysis showed that the characteristics of the swims induced by light dimming were qualitatively different between *prs* and wild-type larvae (Fig. 6). Specifically, we observed that swims in *prs* mutant larvae in response to light dimming were significantly less tortuous than those in wild-type larvae. This difference in tortuosity is evident in projection images of the swimming of wild-type and *prs* larvae induced by light dimming in Movie 1 (Fig. 6A,B), and in the quantification of swim tortuosity (Fig. 6C). Moreover, we observed the same change in tortuosity in the dimming responses of the *C. savignyi* albino mutants *spt* and *imm* versus wild-type *C. savignyi* larvae (Fig. S3). Thus in albino larvae, in which pigment is lost from the Group I photoreceptors, we observed both an increase in the percentage of larvae responding to light dimming and a decrease in the tortuosity of the resulting swims.

Transient inhibition of symmetrical swimming in response to light dimming

While the above analysis of the dimming response involved larvae which were stationary at the time of light dimming, we observed a different response in wild-type larvae that were already swimming when the lights were dimmed. In this case, we observed that the larvae abruptly reversed direction at lights out, and then returned to symmetrical swimming within ∼0.6 s (Fig. 7; Movie 7). Fig. 7A shows the trajectories of the five larvae which were already swimming at the moment of light dimming in Movie 7, both before (orange lines) and after lights-off (blue lines). Fig. 7B shows a compilation of all similar swims (22 total) from five movies. Of these swims, 17 showed trajectory reversals at lights-off (left), while five did not. As with the stationary larvae, the majority (14 out of 17) turned counter-clockwise at lights-off (yellow circles in Fig. 7B). Thus, the dimming response is able to inhibit, albeit transiently, the symmetrical swimming pathway. This abrupt change of course, like the highly tortuous swimming induced in stationary larvae, may serve to confuse predators. Interestingly, this behavior was reported over 90 years ago in studies of the dimming response behavior in larvae of the ascidian *Amaroucium pellucidum* (Mast, 1921). It was reported that ‘active specimens’ (i.e. larvae already swimming at time of light dimming) ‘respond by changing their direction of locomotion’.

DISCUSSION

In this study, we focused on the responses of *Ciona* larvae to various illumination conditions inspired by previous descriptions of the larval ascidian dimming and phototactic responses (Svane and Young, 1989; Zega et al., 2006; Tsuda et al., 2003a,b; Horie et al., 2008a,b; Mast, 1921; McHenry, 2005; McHenry and Strother, 2003; Tsuda et al., 2003a,b) and the recently published *C. intestinalis* connectome (Ryan et al., 2016). The phototaxis and dimming response have often been considered to be manifestations of a single behavioral response (e.g. Zega et al., 2006; Sakurai et al., 2004; Mast, 1921; McHenry, 2005), and even when described as distinct behaviors, the swim properties of the two behaviors have not been compared or quantified. Based on the findings reported here, we conclude that the dimming response and negative phototaxis are separate and unique behaviors which have different developmental profiles, that they result in distinct patterns of locomotion, that they serve different purposes and, finally, that they appear to involve different sets of photoreceptors.

Negative phototaxis

The purpose of negative phototaxis in ascidian larvae has been discussed previously, and most likely serves to promote downward swimming (Svane and Young, 1989; Tsuda et al., 2003a,b; Mast, 1921; McHenry, 2005). Directional screening of photoreceptors by pigment combined with casting of the body in the light field is a widely employed mechanism for detecting the direction of light, particularly in animals with a single photoreceptor spot (Nilsson, 2009; Randel and Jékely, 2016). Thus, it seems safe to assume that the Group I photoreceptors of *Ciona*, which project their outer segments into the ocellus pigment cell, are primarily tasked with detecting light direction, and thus are used for negative phototaxis. Accordingly, we observed that the *prs* mutant larvae are able to respond to light but do not show negative phototaxis. We also observed possible casting behaviors preceding phototactic swims in *Ciona*. For example, the larvae exhibiting a sustained swim in Movie 4 can be observed to first swim to face the directional light and then quickly turn away and begin a sustained swim, consistent with the cue to commence sustained swimming being the reduction in illumination on the Group I photoreceptors as the larva turns away from the light. Moreover, because negative phototaxis was observed over a wide range of illumination intensities (Fig. 1), the taxis mechanism appears to be sensitive to the changes in photoreceptor illumination caused by casting, rather than absolute light levels.

Journal of Experimental Biology (2018) 221, jeb177972. doi:10.1242/jeb.177972

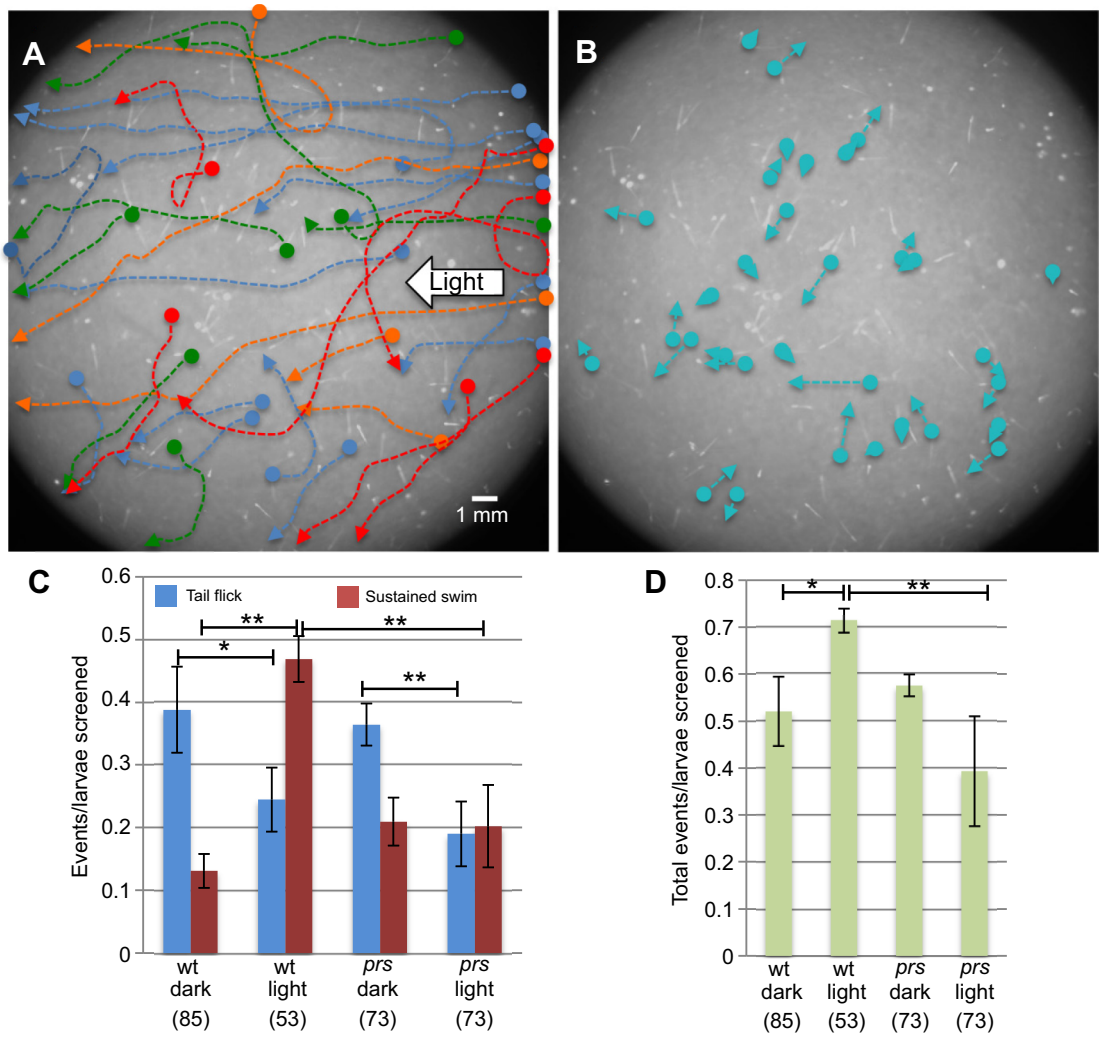

Fig. 4. Swim types in *C. robusta* phototaxis. (A,B) Swim paths in ∼28 hpf *C. robusta* larvae responding to direction of light (indicated). Lines show all swims recorded in a 1 min capture session at 10 frames s^{-1}, and classified as sustained swims (A), or tail flicks (B). (C) Quantification of swims classified as either sustained or tail flicks for wild-type (wt) and homozygous *pristine* mutant (*prs*) larvae either with directional (light) or far-red (dark) illumination. Bars indicate means from three movies (±s.d.). (D) Total swim events. These numbers were generated by summing sustained swims and tail-flick counts from data in C. The total number of larvae screened for each condition (*n*) is given in parentheses in C and D. **P*<0.05, ***P*<0.01 (Student's *t*-test).

The late onset of negative phototaxis, occurring several hours after hatching, may be tied to the diurnal developmental cycle of *Ciona* in which gametes are spawned in the morning in response to the rising sun (Yamaguchi, 1970). The larvae then hatch ∼20 h after fertilization – although the precise timing is temperature dependent. In the first few hours following hatching, both *C. robusta* and *C. intestinalis* larvae are characterized by highly tortuous swimming with no obvious phototaxis despite the presence of directional light cues. This circular swimming then gives way to symmetrical phototaxic swimming. Nevertheless, the swimming response to dimming light remains highly asymmetrical even after the onset of phototaxis, suggesting that these two behaviors serve different purposes and that they involve different visuomotor circuits.

The minimal circuit linking photoreceptors and motor neurons detailed by the 21 hpf *C. intestinalis* connectome predicts a highly asymmetrical, left-biased, activation of motor neurons by both the Group I and Group II photoreceptors (Ryan et al., 2016). Both classes of photoreceptors synapse primarily to posterior BV neurons termed relay neurons (RNs), which in turn send their axons to the MG (Fig. 8). The Group II photoreceptors synapse exclusively with a group of RNs known as the photoreceptor-ascending MG neuron relay neurons (prAMG-RNs). These eight relay neurons are distinguished from the photoreceptor relay neurons (prRNs) by receiving ascending input from the ascending MG peripheral interneurons (AMG) cells of the MG. In contrast, the Group I photoreceptors synapse with both the prAMG-RNs and the six prRNs, as well as with a group of 10 photoreceptor interneurons (prINs) that in turn synapse onto the prRNs. There are three additional RNs that receive dual input from photoreceptors and coronet neurons, and two that receive input from bipolar tail neurons and photoreceptors (not shown in Fig. 8). In the MG, the RNs synapse on the right and left paired (3 on each side) motor ganglion interneurons (MGINs), which in turn make synaptic connections to 10 bilaterally paired motor neurons. In the connectome, the leftward bias is evident in the number and strength of synaptic connections from both the prAMG-RNs and prRNs to the left MGINs. This leftward bias thus may account for the left-biased circular swimming behavior observed in response to light dimming at all larval stages studied, and for the circular swimming behavior of larvae in continuous light for the first few hours following hatching.

Journal of Experimental Biology (2018) 221, jeb177972. doi:10.1242/jeb.177972

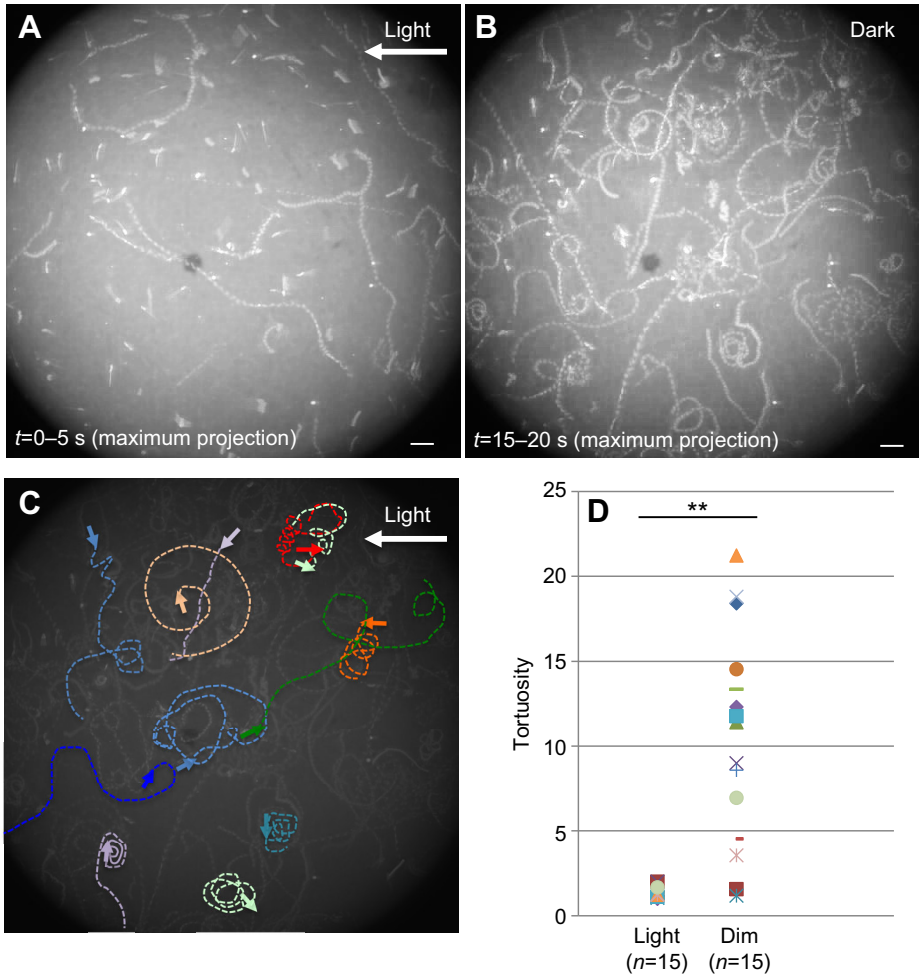

Fig. 5. Phototaxis and dimming behaviors have different swim patterns. (A) Five-second projection images of a field of *C. robusta* larvae in the presence of directional light (arrow). Swims appear as white trails. (B) Same field of view as in A, but showing a 5 s projection of swims following light dimming. Scale bars: (A,B) 1 mm. (C) Selected swim paths of 11 larvae in the 10 s following light dimming. Arrows indicate the orientations of the larvae relative to the indicated directional light at the moment of dimming (anterior at the arrowhead). (D) Quantification of swim tortuosity of larvae before (light) and after (dim) dimming of directional light. The number of swims analyzed (*n*) is indicated. ***P*<0.01 (Wilcoxon signed rank test).

Accordingly, we predict a change(s) in the pathways associated with phototaxis in older larvae. Kajiwara and Yoshida (1985) described developmental changes in the ocellus pigment cell morphology occurring in the 3.5 h following hatching in *C. savignyi* grown at 21°C that correlated with the onset of negative phototaxis. While this mechanism may explain the inability of larvae to detect light direction early after hatching, additional changes to the visuomotor pathway are likely necessary to explain the onset of symmetrical swimming. While this could result from changes in connectivity of the prRNs to the MGINs, other possible mechanisms include new synapses from the photoreceptors to other RNs, such as the antennae RNs, which are highly right-biased. Alternatively, the changes may reflect development or alteration of the central pattern generator (CPG), a fundamental driver of rhythmic motor patterns such as symmetrical swimming (Katz, 2016). A central component of the *Ciona* CPG is thought to be the paired bilateral GABAergic/glycinergic ACIN neurons (two on each side) of the MG described in *C. robusta*, which extend their axons contralaterally (Horie et al., 2010; Nishino et al., 2010). Interestingly, the 21 hpf *C. intestinalis* connectome shows two ACINs on the left side, but only one on the right, and the single right ACIN, despite sending an axon contralaterally, fails to synapse to the left neuropil (Ryan et al., 2016). While these observations may reflect species differences, it is also possible that this represents a developmental difference. Because the precise age of larvae is difficult to assess in publications, and because our results suggest that *C. intestinalis*

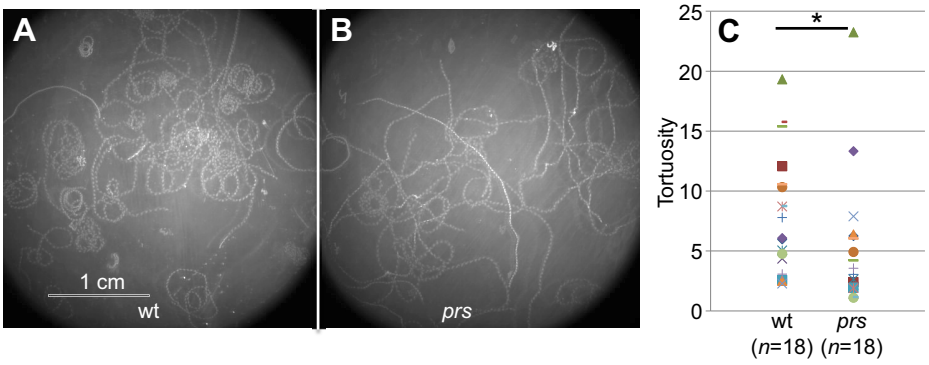

Fig. 6. Dimming response in pristine (*prs*) larvae. (A,B) Ten-second projection images of swims induced by light dimming in wt and *prs* larvae, respectively. (C) Quantification of tortuosity in swims induced by light dimming in wt and *prs* larvae randomly selected from four movies. The total number of swims analyzed (*n*) is indicated. **P*<0.05 (Wilcoxon signed rank test).

Journal of Experimental Biology (2018) 221, jeb177972. doi:10.1242/jeb.177972

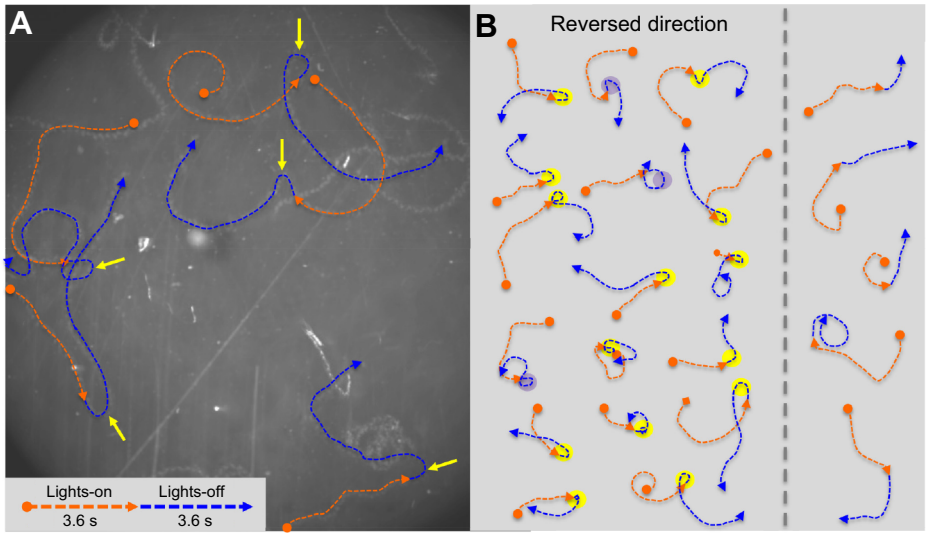

Fig. 7. Trajectory reversal induced by light dimming in swimming larvae. (A) Traces of swims from five larvae in Movie 7. Orange lines indicate swims before lights-off, and blue lines indicate swims after lights-off. Yellow arrows indicate trajectory reversals that immediately follow lights-off. (B) Collection of 22 swims from five movies. Swims on the left of the dashed line show trajectory reversals. Turns highlighted in yellow are counter-clockwise and those in purple are clockwise.

may develop more slowly than *C. robusta*, further investigation of development of the *Ciona* CPG may be informative. Thus, it is possible that in the early hatching larva, the absence of the contralateral inhibitory pathway could accentuate asymmetrical inputs, while later development of this pathway could allow for symmetrical swimming.

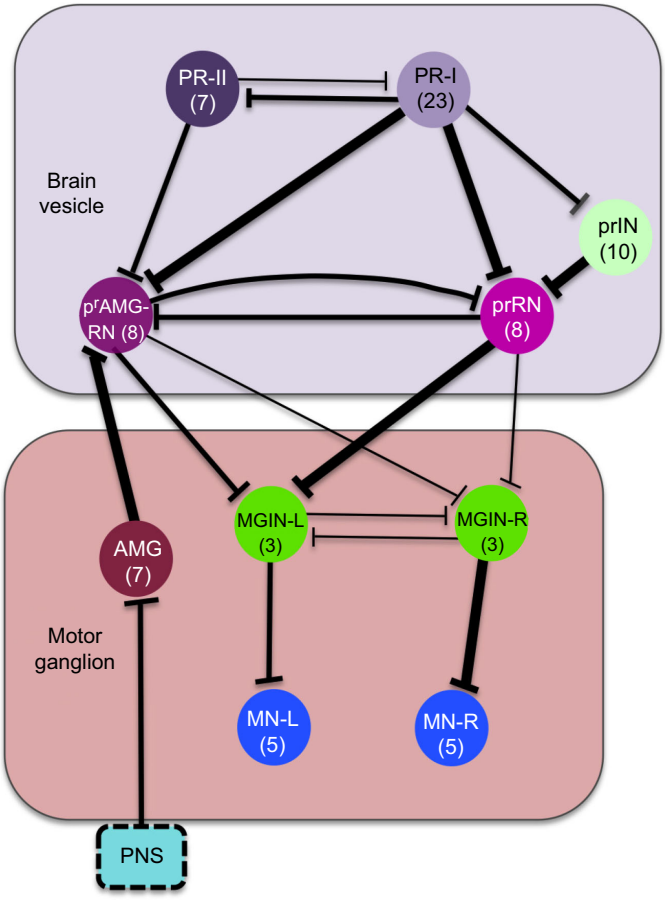

Fig. 8. Minimal visuomotor pathway from 21 hpf *C. intestinalis* larvae. PR-I: Group I photoreceptor; PR-II: Group II photoreceptor; prIN: photoreceptor interneuron; prAMG-RN: photoreceptor-ascending MG neuron relay neuron; prRN: photoreceptor relay neuron; MGIN-L and MGIN-R: motor ganglion interneuron (left and right); AMG: ascending MG peripheral interneuron; MN-L and MN-R: motor neuron (left and right); PNS, peripheral nervous system. The numbers in parentheses indicate the number of cells in that class.

The dimming response

The dimming response behavior of *Ciona* larvae results from the detection of changes in ambient light and is provoked over a wide range of initial illumination intensities (Fig. S1). In contrast to negative phototaxis, which is characterized by oriented symmetrical swims, we observed that light dimming results in circular swimming in stationary larvae and reversals in direction for larvae that are already swimming when the lights are dimmed. Although the majority of the circular swims induced by light dimming appear to be counter-clockwise, the pattern and trajectories of the swims are highly variable. Based on our observations, we propose that the dimming response in *Ciona* larvae functions as an escape mechanism, analogous to the escape mechanism to looming objects observed in both invertebrates and vertebrates (Peek and Card, 2016). Not only is the dimming response distinct from the negative phototaxis response but also the patterns of swimming evoked by light dimming (i.e. circular and/or abrupt changes in direction) are consistent with avoiding predation.

While the Group I photoreceptors with their associated pigment and lens cells appear specialized for detecting the direction of light, we hypothesize that the Group II photoreceptors – because they are not associated with pigment – should be more responsive to changes in ambient illumination, and thus mediate the dimming response, either alone or possibly in conjunction with the Group I photoreceptors. Previous studies have shown that laser co-ablation of the Group I and Group II photoreceptors eliminated the dimming response (Tsuda et al., 2003a,b; Horie et al., 2008a,b). In our studies, we found that the close proximity of the Group I and Group II photoreceptors prevented us from convincingly ablating one group without disrupting the other, and this problem is further complicated by the fact that the axons from the anteriorly situated Group II photoreceptors project posteriorly next to the Group I photoreceptor cell bodies (Ryan et al., 2016). As an alternative approach, we found that observation of the dimming response in albino mutants was informative on photoreceptor activation in this response. Most significantly, we observed that the swims induced by light dimming in the mutants *prs*, *spt* and *imm* were all significantly straighter than those of their wild-type counterparts.

Our interpretation of these observations is that the Group I photoreceptors, which almost certainly are mediating phototaxis, can become sensitive to changes in ambient light by elimination of the shielding pigment. However, because they normally activate the symmetrical pathway, the swims induced by dimming light are straighter. Consistent with this, we observed that *prs* mutant larvae were more sensitive to dimming from low light conditions, suggesting that additional photoreceptors were responding compared with pigmented larvae. These results thus suggest that the Group I photoreceptors normally play little or no role in the dimming response. If *cis*-regulatory elements that drive expression in one photoreceptor group and not the other can be identified, it may be possible to further refine this model. Alternatively, selective illumination of the photoreceptor types could be informative.

The observation that the exclusive RNs of the Group II photoreceptors are the prAMG-RNs further supports their role in the dimming response (Fig. 8). The primary inputs to the AMGs are not from within the MG but rather are from the PNS (Ryan et al., 2018, 2016), including peripheral nerves themselves (most prominently, the posterior apical trunk epidermal neurons), and interneurons of the PNS circuit including the eminens neurons and the ddN cells, the latter of which have been equated with the startle response-mediating vertebrate Mauthner cells (Hale et al., 2016). Thus, this connection to the PNS may link the prAMG-RNs, and by association the Group II photoreceptors, to the proposed *Ciona* startle-response pathway (Ryan et al., 2017), suggesting that prAMG-RNs may serve as part of an integrated escape mechanism.

The course reversals observed of swimming larvae in response to light dimming (Fig. 7) imply that the asymmetrical pathway is able to transiently override or inhibit the symmetrical pathway. Starting from the photoreceptors, there are numerous places this inhibition could take place (Fig. 8). While the majority of the Group II photoreceptors appear to be glutamatergic (Horie et al., 2008a,b), there are also reports of GABAergic photoreceptors (Zega et al., 2008), and judging from the published *in situ* hybridization results the GABAergic photoreceptors appear to be in the anterior group of photoreceptors (i.e. Group II), suggesting a possible inhibitory pathway. In addition, there are numerous GABAergic neurons in the posterior BV where the photoreceptor RNs are clustered (Yoshida et al., 2004), and extensive synaptic contacts are made both within RN types and between the prAMG-RNs and the prRNs (Fig. 8), suggesting an alternative inhibitory pathway. Finally, the dopamine-expressing coronet cells have been suggested to be a negative modulator of the dimming response, although this appears to be mediated through an α2 adrenergic receptor rather than a dopamine receptor, which is not present in the *Ciona* genome (Razy-Krajka et al., 2012). Crosstalk between coronet and photoreceptor pathways is found both at shared relay neurons in the brain vesicle and at common target cells in the motor ganglion (Ryan et al., 2016). A fuller characterization of neurotransmitter and receptor expression at cellular resolution should help clarify the *Ciona* larval neural circuitry, and allow for better comparison with other simple visuomotor circuits, such as those found in larval *Drosophila* (Larderet et al., 2017) and *Platynereis* (Randel et al., 2014).

Relationship of *Ciona* visuomotor responses to those of vertebrates

The types of light-provoked behaviors described here, phototaxis and the dimming/shadow response, are widespread throughout the metazoans (Nilsson, 2009; Randel and Jékely, 2016; Peek and Card, 2016), including vertebrate larvae (Chen and Engert, 2014; Temizer et al., 2015). Because of the useful information contained in such environmental cues as light direction and changes in ambient light, it is not surprising that these behaviors are nearly ubiquitous, and it is likely that the repertoire of similar behaviors shared among animals reflects both divergent and convergent pathways of evolution. More significant may be the possible conservation of visuomotor pathways and mechanisms between ascidians and vertebrates due to their relatively recent common ancestry. Ascidian photoreceptors themselves show strong affinity to vertebrate ciliary photoreceptors, rather than the rhabdomeric type of most invertebrates (Kusakabe and Tsuda, 2007; Lamb et al., 2007), and are hyperpolarizing like those of vertebrates (Eakin and Kuda, 1971). However, possible relationships of other components of the ascidian visuomotor response (e.g. RNs) to vertebrate retinal cells (e.g. bipolar and ganglion cells) and processing centers (e.g. optic tectum) remain to be determined.

Acknowledgements

We thank Takehiro Kusakabe for anti-arrestin antibody.

Competing interests

The authors declare no competing or financial interests.

Author contributions

Conceptualization: P.S., W.C.S.; Methodology: W.C.S.; Validation: W.C.S.; Formal analysis: P.S., V.V., E.N., M.J.K., W.C.S.; Investigation: P.S., V.V., E.N., M.J.K., W.C.S.; Data curation: P.S.; Writing - original draft: W.C.S.; Writing - review & editing: P.S., V.V., E.N., M.J.K., W.C.S.; Supervision: W.C.S.; Project administration: W.C.S.; Funding acquisition: W.C.S.

Funding

This work was supported by a seed grant from CalBRAIN (California Blueprint for Research to Advance Innovations in Neuroscience), and National Institutes of Health awards HD038701 and NS103774. Deposited for release in PMC after 12 months.

Supplementary information

Supplementary information available online at
http://jeb.biologists.org/lookup/doi/10.1242/jeb.177972.supplemental

References

Brunetti, R., Gissi, C., Pennati, R., Caicci, F., Gasparini, F. and Manni, L. (2015). Morphological evidence that the molecularly determined Ciona intestinalis type A and type B are different species: Ciona robusta and Ciona intestinalis. *J. Zool. Syst. Evol. Res.* **53**, 186-193.

Caputi, L., Andreakis, N., Mastrototaro, F., Cirino, P., Vassillo, M. and Sordino, P. (2007). Cryptic speciation in a model invertebrate chordate. *Proc. Natl. Acad. Sci. USA* **104**, 9364-9369.

Chen, X. and Engert, F. (2014). Navigational strategies underlying phototaxis in larval zebrafish. *Front. Syst. Neurosci.* **8**, 39.

Delsuc, F., Brinkmann, H., Chourrout, D. and Philippe, H. (2006). Tunicates and not cephalochordates are the closest living relatives of vertebrates. *Nature* **439**, 965-968.

Eakin, R. M. and Kuda, A. (1971). Ultrastructure of sensory receptors in Ascidian tadpoles. *Z. Zellforsch. Mikrosk. Anat.* **112**, 287-312.

Grave, C. (1920). Amaroucium pellucidum (Leidy) form constellatum (Verrill) I. The activities and reactions of the tadpole larva. *J. Exp. Zool.* **30**, 239-257.

Hale, M. E., Katz, H. R., Peek, M. Y. and Fremont, R. T. (2016). Neural circuits that drive startle behavior, with a focus on the Mauthner cells and spiral fiber neurons of fishes. *J. Neurogenet.* **30**, 89-100.

Hashimoto, H., Robin, F. B., Sherrard, K. M. and Munro, E. M. (2015). Sequential contraction and exchange of apical junctions drives zippering and neural tube closure in a simple chordate. *Dev. Cell* **32**, 241-255.

Horie, T., Orii, H. and Nakagawa, M. (2005). Structure of ocellus photoreceptors in the ascidian Ciona intestinalis larva as revealed by an anti-arrestin antibody. *J. Neurobiol.* **65**, 241-250.

Horie, T., Sakurai, D., Ohtsuki, H., Terakita, A., Shichida, Y., Usukura, J., Kusakabe, T. and Tsuda, M. (2008a). Pigmented and nonpigmented ocelli in the brain vesicle of the ascidian larva. *J. Comp. Neurol.* **509**, 88-102.

Horie, T., Kusakabe, T. and Tsuda, M. (2008b). Glutamatergic networks in the Ciona intestinalis larva. *J. Comp. Neurol.* **508**, 249-263.

Horie, T., Nakagawa, M., Sasakura, Y., Kusakabe, T. G. and Tsuda, M. (2010). Simple motor system of the ascidian larva: neuronal complex comprising putative cholinergic and GABAergic/glycinergic neurons. *Zoolog. Sci.* **27**, 181-190.

Hudson, C. (2016). The central nervous system of ascidian larvae. *Wiley Interdiscip Rev. Dev. Biol.* **5**, 538-561.
Ikuta, T. and Saiga, H. (2007). Dynamic change in the expression of developmental genes in the ascidian central nervous system: revisit to the tripartite model and the origin of the midbrain-hindbrain boundary region. *Dev. Biol.* **312**, 631-643.
Jiang, D., Tresser, J. W., Horie, T., Tsuda, M. and Smith, W. C. (2005). Pigmentation in the sensory organs of the ascidian larva is essential for normal behavior. *J. Exp. Biol.* **208**(Pt 3), 433-438.
Kajiwara, S. and Yoshida, M. (1985). Changes in behavior and ocellar structure during the larval life of solitary ascidians. *Biol. Bull.* **169**, 565-577.
Katz, P. S. (2016). Evolution of central pattern generators and rhythmic behaviours. *Philos. Trans. R. Soc. Lond. B Biol. Sci.* **371**, 20150057.
Kusakabe, T. and Tsuda, M. (2007). Photoreceptive systems in ascidians. *Photochem. Photobiol.* **83**, 248-252.
Lamb, T. D., Collin, S. P. and Pugh, E. N., Jr (2007). Evolution of the vertebrate eye: opsins, photoreceptors, retina and eye cup. *Nat. Rev. Neurosci.* **8**, 960-976.
Larderet, I., Fritsch, P. M. J., Gendre, N., Neagu-Maier, G. L., Fetter, R. D., Schneider-Mizell, C. M., Truman, J. W., Zlatic, M., Cardona, A. and Sprecher, S. G. (2017). Organization of the Drosophila larval visual circuit. *Elife* **6**.
Mast, S. O. (1921). Reactions to light in the larvae of the ascidians, Amaroucium constellatum and Amaroucium pellucidum with special reference to photic orientation. *J. Exp. Zool.* **34**, 149-187.
Mchenry, M. J. (2005). The morphology, behavior, and biomechanics of swimming in ascidian larvae. *Can. J. Zool.* **83**, 62-74.
McHenry, M. J. and Strother, J. A. (2003). The kinematics of phototaxis in larvae of the ascidian Aplidium constellatum. *Mar. Biol.* **142**, 173-184.
Moret, F., Christiaen, L., Deyts, C., Blin, M., Joly, J.-S. and Vernier, P. (2005). The dopamine-synthesizing cells in the swimming larva of the tunicate Ciona intestinalis are located only in the hypothalamus-related domain of the sensory vesicle. *Eur. J. Neurosci.* **21**, 3043-3055.
Nakagawa, M., Ohkuma, M. and Tsuda, M. (1999). Action spectrum for the photophobic response of Ciona intestinalis (Ascidieacea, Urochordata) larvae implicates retinal protein. *Photochem. Photobiol.* **70**, 359-362.
Nakamura, M. J., Okubo, R., Hotta, K. and Oka, K. (2012). Three-dimensional anatomy of the Ciona intestinalis tailbud embryo at single-cell resolution. *Dev. Biol.* **372**, 274-284.
Nilsson, D.-E. (2009). The evolution of eyes and visually guided behaviour. *Philos. Trans. R. Soc. Lond. B Biol. Sci.* **364**, 2833-2847.
Nishino, A., Okamura, Y., Piscopo, S. and Brown, E. R. (2010). A glycine receptor is involved in the organization of swimming movements in an invertebrate chordate. *BMC Neurosci.* **11**, 6.
Peek, M. Y. and Card, G. M. (2016). Comparative approaches to escape. *Curr. Opin. Neurobiol.* **41**, 167-173.
Randel, N. and Jékely, G. (2016). Phototaxis and the origin of visual eyes. *Philos. Trans. R. Soc. Lond. B Biol. Sci.* **371**, 20150042.
Randel, N., Asadulina, A., Bezares-Calderón, L. A., Verasztó, C., Williams, E. A., Conzelmann, M., Shahidi, R. and JéKely, G. (2014). Neuronal connectome of a sensory-motor circuit for visual navigation. *Elife* **3**.
Razy-Krajka, F., Brown, E. R., Horie, T., Callebert, J., Sasakura, Y., Joly, J.-S., Kusakabe, T. G. and Vernier, P. (2012). Monoaminergic modulation of photoreception in ascidian: evidence for a proto-hypothalamo-retinal territory. *BMC Biol.* **10**, 45.
Ryan, K., Lu, Z. and Meinertzhagen, I. A. (2016). The CNS connectome of a tadpole larva of Ciona intestinalis (L.) highlights sidedness in the brain of a chordate sibling. *Elife* **5**.
Ryan, K., Lu, Z. and Meinertzhagen, I. A. (2017). Circuit homology between decussating pathways in the ciona larval CNS and the vertebrate startle-response pathway. *Curr. Biol.* **27**, 721-728.
Ryan, K., Lu, Z. and Meinertzhagen, I. A. (2018). The peripheral nervous system of the ascidian tadpole larva: types of neurons and their synaptic networks. *J. Comp. Neurol.* **526**, 583-608.
Sakurai, D., Kohmura, Y., Horie, T., Iwamoto, H., Ohtsuki, H. and Tsuda, M. (2004). The role of pigment cells in the brain of ascidian larva. *J. Comp. Neurol.* **475**, 70-82.
Satoh, N. (1994). *Developmental Biology of Ascidians. Developmental and Cell Biology Series*, Vol. xv, 234 p, 2 p. of plates. Cambridge England; New York: Cambridge University Press.
Satoh, N. (2014). *Developmental Genomics of Ascidians*, Vol. xi, 201 pages. Hoboken, New Jersey: Wiley Blackwell.
Schneider, C. A., Rasband, W. S. and Eliceiri, K. W. (2012). NIH Image to ImageJ: 25 years of image analysis. *Nat. Methods* **9**, 671-675.
Stolfi, A., Ryan, K., Meinertzhagen, I. A. and Christiaen, L. (2015). Migratory neuronal progenitors arise from the neural plate borders in tunicates. *Nature* **527**, 371-374.
Svane, I. B. and Young, C. M. (1989). The ecology and behavior of ascidian larvae. *Mar. Biol. Rev.* **27**.
Temizer, I., Donovan, J. C., Baier, H. and Semmelhack, J. L. (2015). A visual pathway for looming-evoked escape in larval zebrafish. *Curr. Biol.* **25**, 1823-1834.
Tsuda, M., Kawakami, I. and Shiraishi, S. (2003a). Sensitization and habituation of the swimming behavior in ascidian larvae to light. *Zoolog. Sci.* **20**, 13-22.
Tsuda, M., Sakurai, D. and Goda, M. (2003b). Direct evidence for the role of pigment cells in the brain of ascidian larvae by laser ablation. *J. Exp. Biol.* **206**, 1409-1417.
Veeman, M. T., Chiba, S. and Smith, W. C. (2011). Ciona genetics. *Methods Mol. Biol.* **770**, 401-422.
Yamaguchi, M. (1970). Spawning periodicity and settling time in ascidians, Ciona intestinalis and Styela plicata. *Rec. Oceanogr. Wks.* **10**, 147-155.
Yoshida, R., Sakurai, D., Horie, T., Kawakami, I., Tsuda, M. and Kusakabe, T. (2004). Identification of neuron-specific promoters in Ciona intestinalis. *Genesis* **39**, 130-140.
Young, C. M. and Chia, F.-S. (1985). An experimental test of shadow response function in ascidian tadpoles. *J. Exp. Mar. Biol. Ecol.* **85**, 165-175.
Zega, G., Thorndyke, M. C. and Brown, E. R. (2006). Development of swimming behaviour in the larva of the ascidian Ciona intestinalis. *J. Exp. Biol.* **209**(Pt 17), 3405-3412.
Zega, G., Biggiogero, M., Groppelli, S., Candiani, S., Oliveri, D., Parodi, M., Pestarino, M., De Bernardi, F. and Pennati, R. (2008). Developmental expression of glutamic acid decarboxylase and of gamma-aminobutyric acid type B receptors in the ascidian Ciona intestinalis. *J. Comp. Neurol.* **506**, 489-505.

Supplemental material

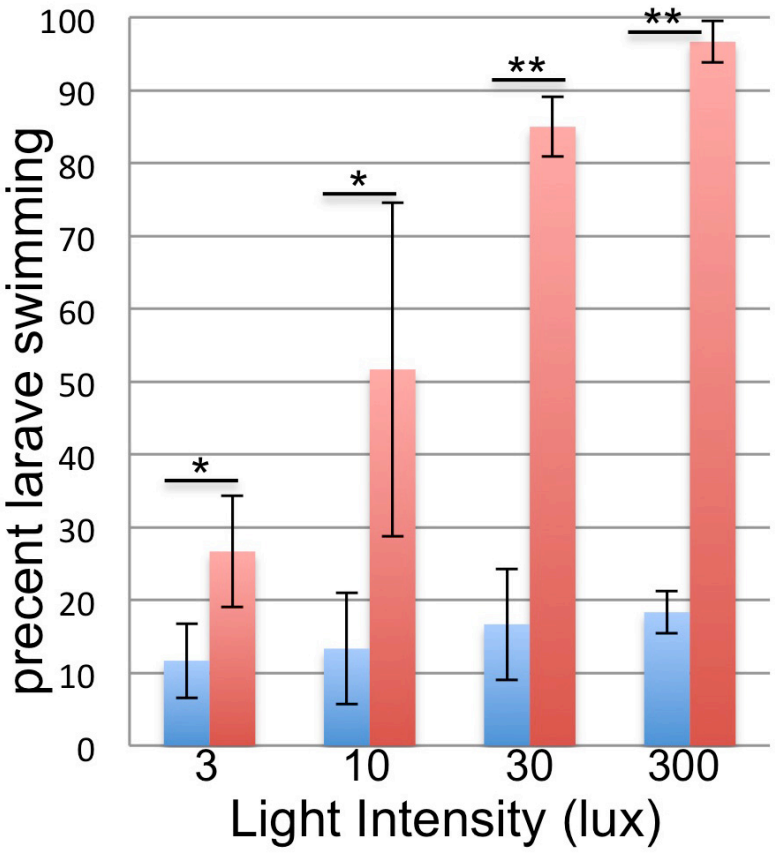

Figure S1. Dimming response of wild type Ciona robusta larvae as a function of light intensity (lux). Blue bars indicate the percentage of larvae swimming in a 5-second period prior to dimming, while red bars indicate percentage of larvae swimming in a 5-second period after dimming. Shown are the averages from three movies with 20 larvae assessed for each movie (± S.D). * P<0.05, **P<0.01.

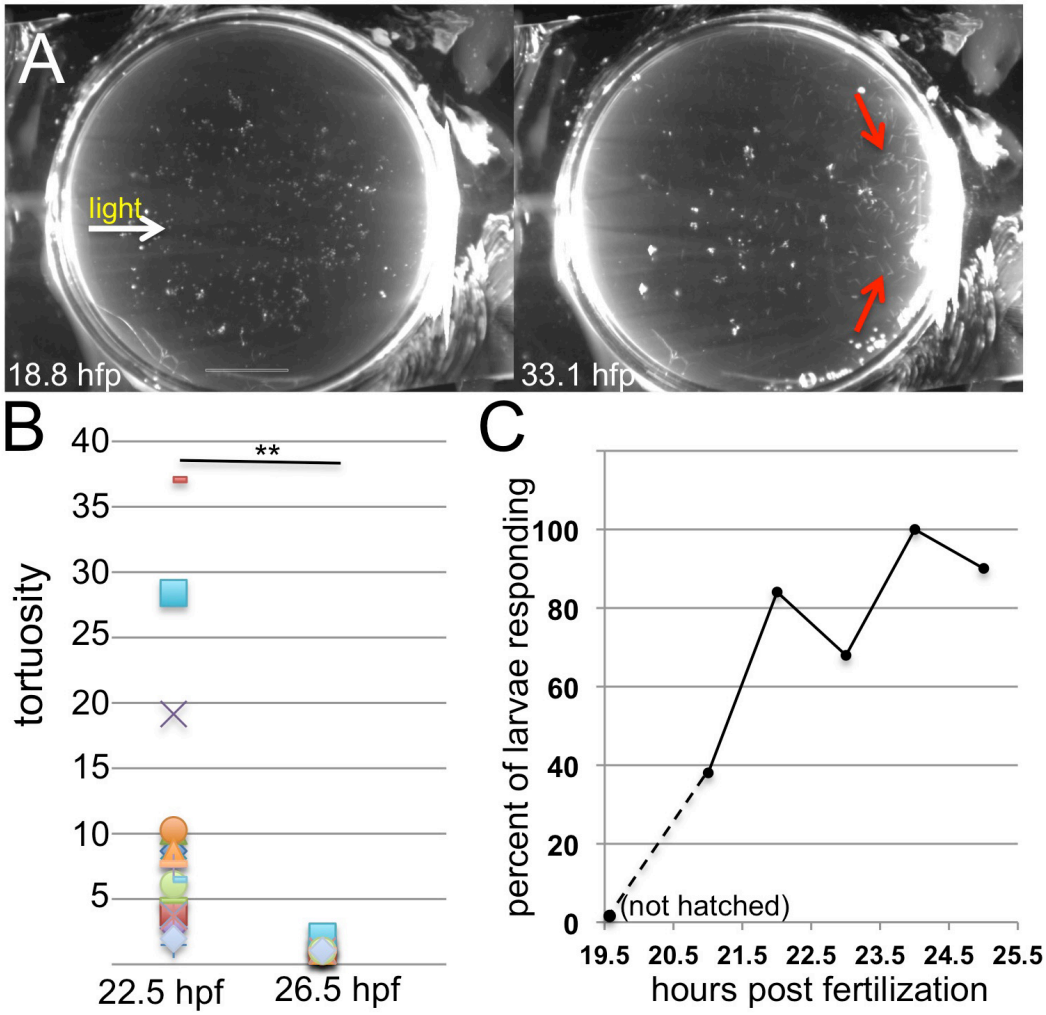

Figure S2. **A**. Negative phototaxis of *Ciona intestinalis* larvae at the beginning and end points of the assay (18.8 and 33.1 hpf). Arrow in left panel indicates the direction of light, and red arrows in right panel indicate accumulation of larvae at the side of the dish away from the light. **B.** Relative tortuosity of swims of *C. intestinalis* larvae in continuous directional light. Developmental times are indicated. **P<0.01 (Wilcoxon signed rank test). **C.** Developmental time course of the dimming response in *C. intestinalis* presented as a percent of larvae responding to dimming light.

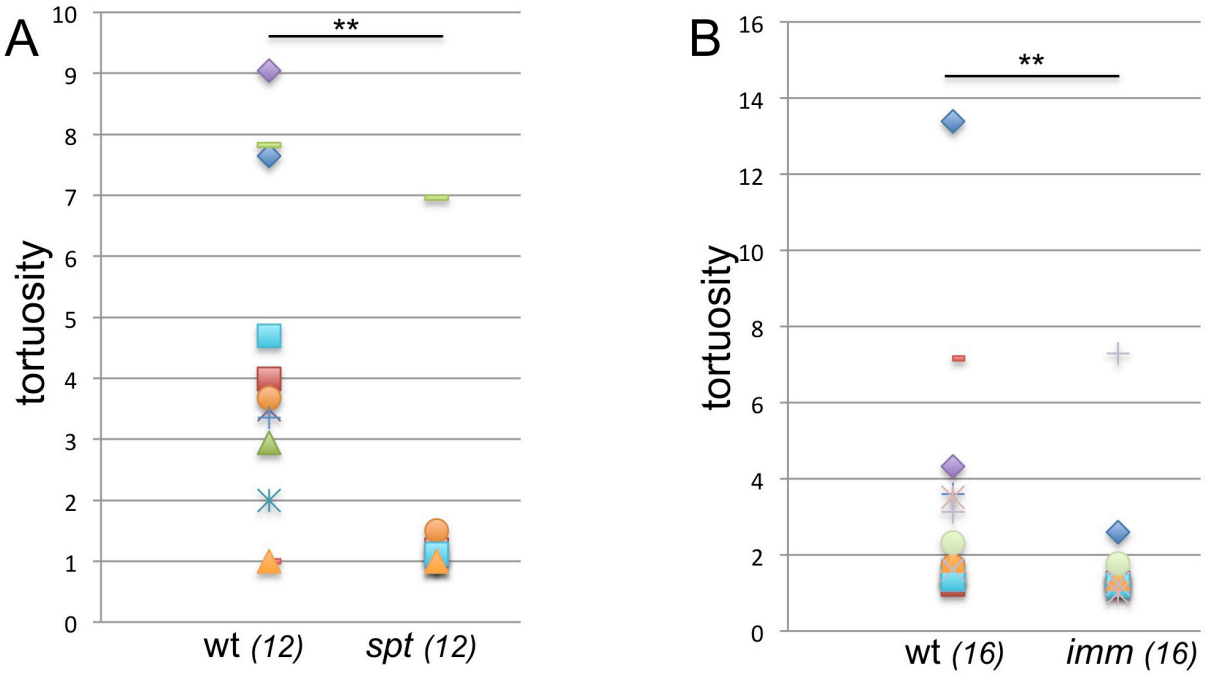

Figure S3. Quantification of swim tortuosity of dimming response swims in *Ciona savignyi* wt and albino larvae. Comparisons of wt to larvae homozygous for the *spotless* (*spt*) **(A)** and to the *immaculate* (*imm*) mutations **(B)**. Number of swims analyzed are in parentheses. **P<0.01 (Wilcoxon signed rank test).

Movie 1. Dimming response of wild type and *pristine* larvae. This thirty second movie, captured at 10 frames per second, is shown at 5-times normal speed. Dimming is evident at the midpoint of the movie. Bar in frame one equals 1 cm.

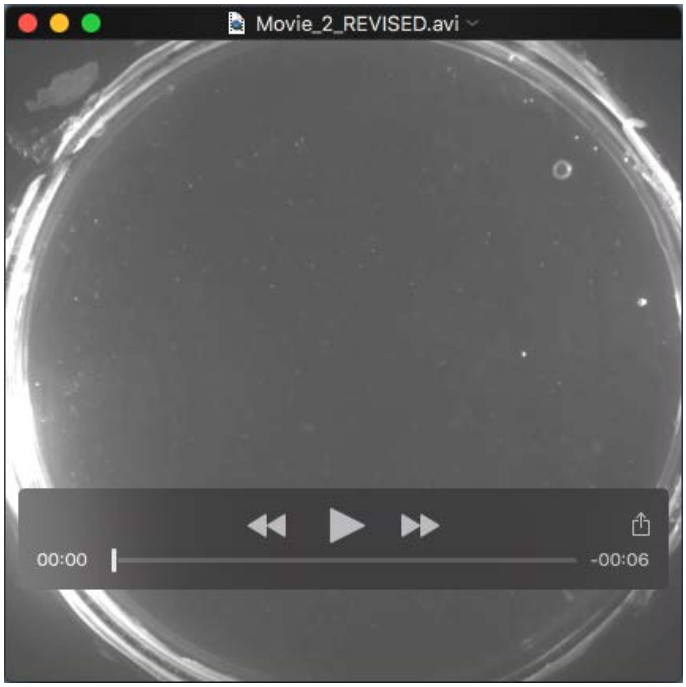

Movie 2. Negative phototaxis of *C. robusta* larvae. Movie shows an elapsed time of 11.8 hours captured at one frame per 10 minutes. Directional light is from the right.

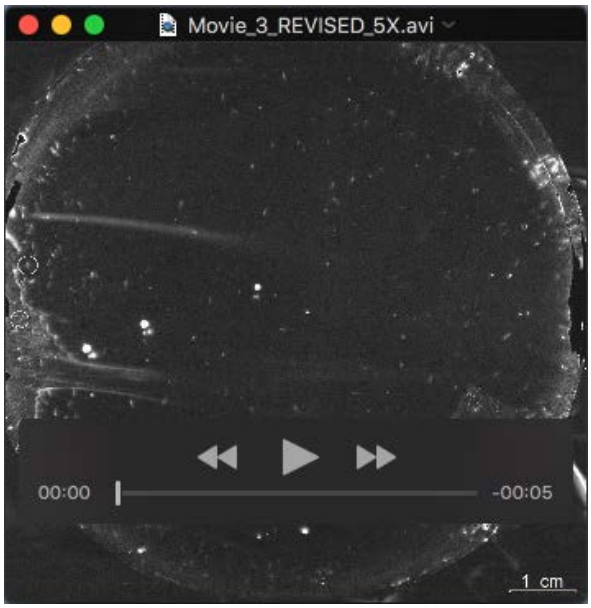

Movie 3. Negative phototaxis of *C. robusta* larvae at 25 hours post fertilization. Circled larvae display sustained negative phototaxic swims. Directional light is from the left. This thirty second movie, captured at 10 frames per second, is shown at 5-times normal speed.

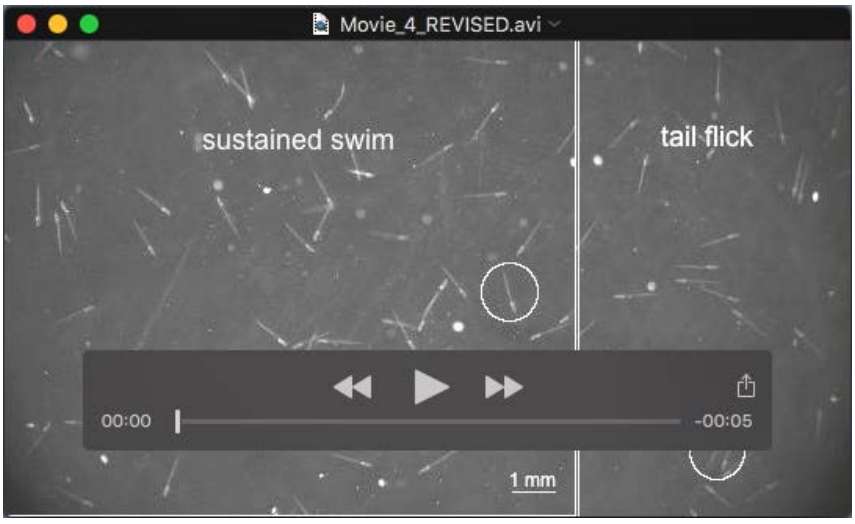

Movie 4. Examples of sustained swims and tail flick. Images captured at 10 frames per second.

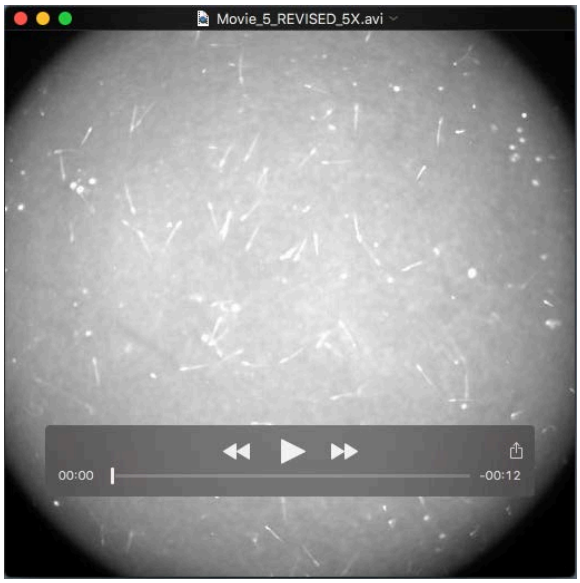

Movie 5. Larvae (~28 hpf) displaying negative phototaxis. Directional light is from the right. Movie is shown at 5 times normal speed.

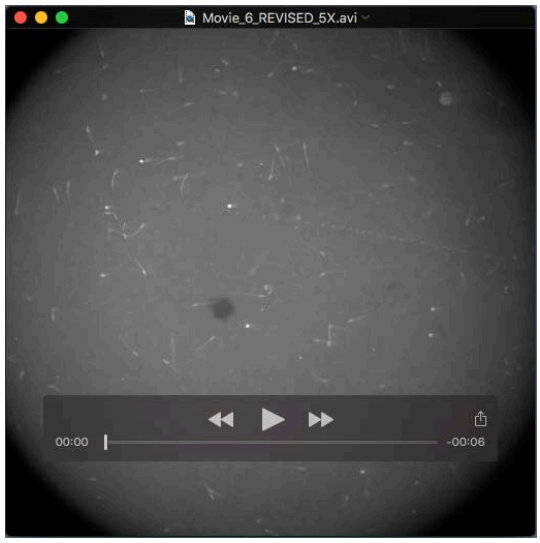

Movie 6. Response of larvae to dimming of directional light. Light dimming is evident at midpoint of this 30 second movie, shown here at 5 times normal speed. Directional light is from the left.

Journal of Experimental Biology • Supplementary information

Movie 7. Response of swimming larvae to dimming light. Two larvae showing swim-trajectory reversals at light dimming are circled.